A neural approach to unsupervised classification of very-high resolution polarimetric SAR data

www.geok.it

Alessandro Burini*, Cosimo Putignano*, Fabio Del Frate, Marco Del Greco**, Giovanni Schiavon** and Domenico Solimini****

**GEO-K srl, Rome, Italy (alessandro.burini@geok.it)*

***Department of Computer Science, Systems and Production , Tor Vergata University, Rome, ITALY (schiavon@disp.uniroma2.it)*

Introduction

The performance of space borne Synthetic Aperture Radars is being expanded by the new generation missions, which are beginning to make available polarimetric data, till now provided by airborne system. This kind of data are expected to be useful for a number of land applications, including discrimination among different kinds of surfaces and objects.

We develop and implement a controlled maximum-distance Self-Organizing Map (SOM) for the identification of the scattering mechanisms present in the observed pixels and effectively assess their strength.

Goals

Our aim is to test the SOM methodology for very-high resolution (~2 m) L-band polarimetric SAR images of an undulating, heterogeneous and fragmented landscape.

Data Set

The images were acquired in the fall of 2005 within the Bacchus DOC campaign supported by ESA. The E-SAR Synthetic Aperture Radar system onboard the DLR Dornier DO 288 aircraft overflow the Frascati test site in the Colli Albani area, SE of Rome, Italy, on 5 and 25 October. The study area was imaged at very high spatial resolution at L-band in a fully polarimetric mode and at two incidence angles. The site of interest was covered by two strips 3 km x 7 km each. The main land classes consist of urbanized and agricultural surfaces. These latter include vineyards, olive groves, maize and grassy soil.

Contemporarily to each SAR acquisition, intensive and extensive *in situ* observations were carried out by the Tor Vergata Earth Observation Laboratory staff to built up a georeferenced ground truth database. The following analysis refers to the image acquired on 25 October at 40 degrees incidence angle (at the center of the swath).

Methodology

After the calibration, which takes into account the variability of the local incidence angle α (DEM corrected, Fig. 1)

$$\sigma_0 = 20\log DN - 60 + 10\log(sen\alpha)$$

a new image has been synthesized from the SLC polarimetric data, by attributing a 9-components vector to each pixel. The components are standard polarization combinations:

$$[x]_{i,j} = \begin{bmatrix} HH \\ HV \\ VV \\ RR \\ RL \\ LL \\ Lin_{45°}Lin_{45°} \\ Lin_{45°}Lin_{135°} \\ Lin_{135°}Lin_{135°} \end{bmatrix}_{i,j}, \quad \text{where} \quad \begin{array}{l} i = 1,\cdots,n\_lines \\ j = 1,\cdots,n\_samples \end{array}$$

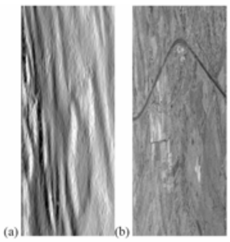

Figure 1. Local incidence angle α variation (a) and the corresponding DEM corrected image (b).

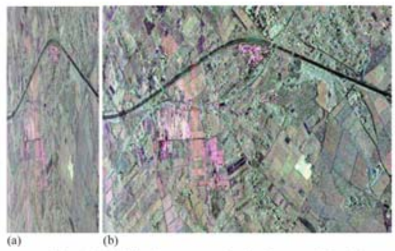

Figure 2. Multilook pre-processing: before (a) and after (b). Red: HH; green: HV; blue: VV.

Now a self-organizing neural network fed by the 9-components vectors, transforms the nonlinear statistical relationships among the high-dimensional data of the image in Fig. 2b onto an organized two-dimension map.

$$y_j = \sum_{i=1}^{n} w_{ij} x_i \,,$$

where $\underline{x} = [x_1, \; x_2, \; \ldots, \; x_n]^T$,
$\underline{w}_j = [w_{j1}, \; w_{j2}, \; \ldots, \; w_{jn}]^T$, $\underline{y} = [y_1, \; y_2, \; \ldots, \; y_m]^T$

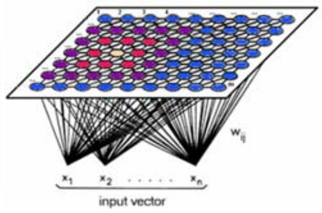

Classification, results and conclusions

Three regions are visible in the U-Matrix representation of the map. Each region of closely packed neurons corresponds to a principal scattering mechanism (PSM) and is separated from the others by stripes of more distant neurons.

It is important to note that the PSM initialization subdivides the two-dimensional map into three balanced, specialized and stable areas.

Figure 4. U-Matrix representation of the SOM.

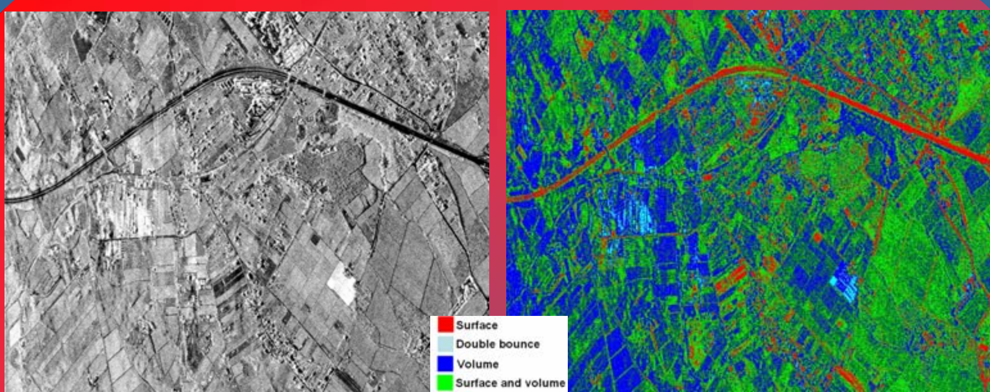

A check against the intensive and extensive ground truth points out an excellent discrimination capability over the test area. For instance, the pixels of the freeway lanes and of the secondary roads not screened by vegetation are correctly attributed to the pure surface scattering class. The buildings in the central upper part of the image are prevalently identified as pixels with a double-bounce mechanism. The pixels of the agricultural crops are subdivided into a class of pure volume scattering and another containing a mix of volume and surface scattering. This discrimination corresponds essentially to the different crop biomass per unit area and plant alignment.

Data were provided by DLR within ESRIN Contract No. 19188/05/I-LG. The support of ESA/ESRIN is gratefully acknowledged